J. Phys.: Condens. Matter **19** (2007) 346236 (11pp) doi:10.1088/0953-8984/19/34/346236

Luminescence of YbP_3O_9 upon excitation in the UV–VUV range

G Stryganyuk[1,2], D Trots[1,3], I Berezovskaya[4], T Shalapska[2], A Voloshinovskii[2], V Dotsenko[4] and G Zimmerer[5]

[1] HASYLAB at DESY, Notkestraße 85, 22607 Hamburg, Germany
[2] Ivan Franko National University of Lviv, 8 Kyryla i Mefodiya Street, 79005 Lviv, Ukraine
[3] Institute for Materials Science, Darmstadt University of Technology, Petersenstrasse 23, 64287 Darmstadt, Germany
[4] Physico-Chemical Institute, Ukrainian Academy of Sciences, 86 Lustdorfskaya doroga, 65080 Odessa, Ukraine
[5] Institute of Experimental Physics, University of Hamburg, Luruper Chaussee 149, 22761 Hamburg, Germany

Received 29 March 2007, in final form 12 July 2007
Published 1 August 2007
Online at stacks.iop.org/JPhysCM/19/346236

Abstract

X-ray powder diffraction and luminescence spectral-kinetic studies have been performed for ytterbium metaphosphate (YbP_3O_9) in the 12–290 K temperature range. The diffraction investigation has shown YbP_3O_9 to be of monoclinic $P2_1/c$ structure at $T = 12$–290 K. Charge transfer luminescence originating from Yb^{3+} ion has been revealed. The carrier confinement within the Yb^{3+} charge transfer state is pronounced at $T = 12$ K. A tendency has been revealed for charge carriers in YbP_3O_9 to be localized in a trapped exciton state at room temperature. The quenching mechanisms for Yb^{3+} charge transfer luminescence and processes competing with the formation of the Yb^{3+} charge transfer state are discussed.

1. Introduction

Crystals of rare-earth (RE) based $Y_{1-x}RE_xP_3O_9$ metaphosphates and their glassy compositions have been studied extensively because of their promising optical properties [1–3]. Ytterbium metaphosphate (YbP_3O_9) reveals a rather high potential concentration of Yb^{3+} ions (5.4×10^{21} cm^{-3}) and a large distance (~5.6 Å) between the nearest Yb^{3+} neighbors [2, 4]. The luminescence in the infrared (~980 nm) range due to the radiative $^2F_{5/2} \rightarrow {}^2F_{7/2}$ transition and the visible (~500 nm) cooperative luminescence (CL) of Yb^{3+} ions [5] were studied for YbP_3O_9 crystal and its glassy compositions. The efficiency of the cooperative interaction for Yb^{3+} ions and concentration quenching of the infrared Yb^{3+} $^2F_{5/2} \rightarrow {}^2F_{7/2}$ emission are reduced in YbP_3O_9 because of the isolation of Yb^{3+} ions from each other [2]. In the present work, a luminescence study of YbP_3O_9 is carried out to clarify the energy transformation

processes upon excitation in the range of Yb^{3+} charge transfer (CT), Yb^{3+} $4f^{13} \rightarrow 4f^{12}5d$, and host absorption.

2. Experiment details

Polycrystalline YbP_3O_9 was grown from a H_3PO_4–NaF flux [2]. A mixture of Yb_2O_3 and P_2O_5 was combined with the flux, preheated to 500 °C for 4 h, held at 950 °C for 10 h, cooled slowly down to 600 °C and quenched.

In situ x-ray diffraction (XRD) investigations have been carried out using the facility of the experimental station B2 [6] at HASYLAB (DESY, Hamburg, Germany). A closed-cycle cryostat [7] was used to reach temperatures in the 12–290 K range. The temperature was fixed at each point during the heating cycle. The diffraction patterns were collected from the sample mounted in the Debye–Scherrer capillary geometry using an image-plate detector [8] (2θ range: 4°–45°). The monochromatic beam was formed using a Si(111) double flat crystal monochromator and a wavelength of 0.498 99 Å was determined after analysis of ten Bragg diffraction maxima from LaB_6 reference material (NIST SRM 660a). Data analysis and all crystallographic calculations (refinement of the lattice parameters, full profile Rietveld structure refinement) were performed using the FullProf programme package [9].

Measurements of luminescence excitation and emission spectra as well as decay kinetics were performed using the facility of the SUPERLUMI station [10] at HASYLAB. The measurements were carried out in the 12–290 K temperature range using a helium-flow-type cryostat. Emission spectra within the 200–1050 nm range were measured with a resolution of 0.5–5 nm using an ARC 'Spectra Pro 300i' 0.3 m monochromator-spectrograph in the Czerny–Turner mounting equipped with a Princeton Instruments CCD detector and a Hamamatsu R6358P photomultiplier. Emission spectra in the vacuum ultraviolet (VUV) range were explored using 0.5 m Pouey-type VUV monochromator equipped with a solar-blind Hamamatsu R6836 photomultiplier and an El-Mul microsphere-plate detector sensitized with caesium iodide. Luminescence excitation spectra were scanned with a resolution of 3.2 Å within the 5–11 eV range by the primary 2 m monochromator in the 15° McPherson mounting. The luminescence decay kinetics were registered within a 200 ns time gate defined by excitation pulse repetition upon storage ring operation in the five-bunch mode. Luminescence excitation spectra have been corrected for the incident photon flux.

3. Results of powder x-ray diffraction study

The diffraction studies were performed with the purpose of clarifying the changes in the YbP_3O_9 structure in the 12–290 K temperature range where the luminescence investigations were carried out. The high-resolution synchrotron x-ray powder diffraction technique was used for this purpose. Phase analysis of the YbP_3O_9 diffraction patterns measured at $T = 290$ K has shown the investigated sample of ytterbium metaphosphate to be free of impurity phases. Analysis of XRD patterns shows that the YbP_3O_9 structure remains monoclinic in the whole temperature range investigated. Rietveld refinement [9] has been performed for the diffraction patterns from the YbP_3O_9 sample using the $P2_1/c$ space group, $Z = 12$ (structure model from [2], ICSD #2132). As examples, the results of Rietveld refinement are presented in figure 1 for the YbP_3O_9 structure at $T = 290$ K (frame (a)) and $T = 12$ K (frame (b)).

The monoclinic structure is characteristic for the REP_3O_9 metaphosphate of RE ions with a small ionic radius [2]. The structure of YbP_3O_9 is depicted in figure 2. Yb^{3+} ions are located inside slightly distorted YbO_6 octahedra that are isolated from each other by corner-sharing PO_4 tetrahedra. The shortest distance between the neighbour Yb^{3+} ions varies from 5.6128(3) Å at

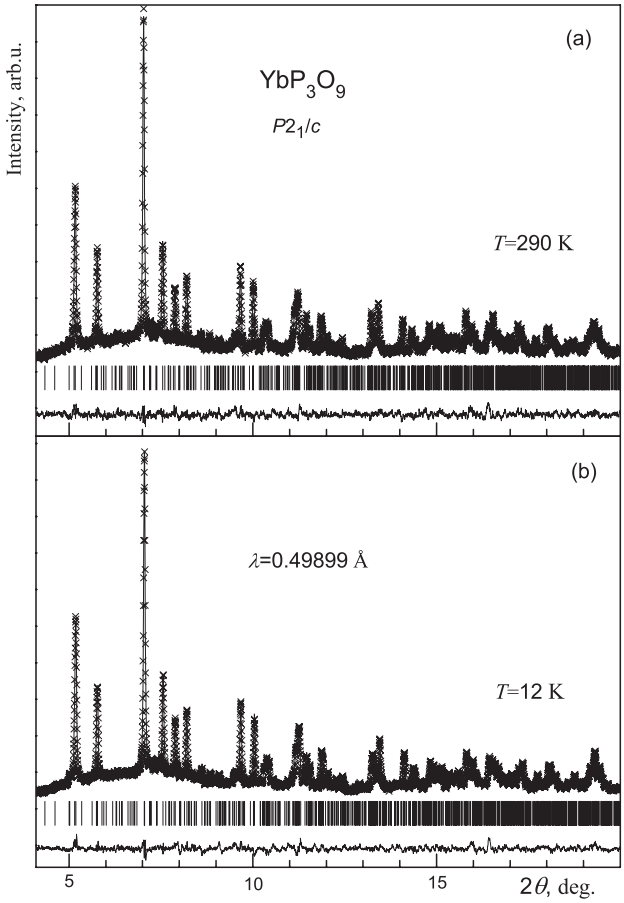

Figure 1. Low-angle region of powder diffraction patterns for ytterbium metaphosphate at $T = 290$ K (frame (a)) and $T = 12$ K (frame (b)). Experimental data (crosses) and the calculated profile (solid line through the crosses) are presented together with the calculated Bragg positions (vertical ticks) and the difference curve (solid line below).

$T = 290$ K down to 5.5981(2) Å at $T = 12$ K. Such a large distance between RE ions in the YbP_3O_9 structure implies a reduced concentration quenching of RE^{3+} emission.

The temperature dependence of YbP_3O_9 lattice parameters is presented in figures 3(a)–(d). The volume of the unit cell (figure 3(e)) increases gradually without any anomalous deviation, while the temperature changes within the 12–290 K range. Thermal changes in cell parameters (a, b, c, β) were fitted using the polynomial $F(T) = A_0 + A_1T^2 + A_2T^3 + A_3T^4$ dependence, and the respective A_i coefficients are presented in table 1. The relative expansion η of the YbP_3O_9 unit cell (figure 3(f)) has been estimated in the 12–290 K range as $\eta x(T) = 100\% \times (x(T) - x(12\ \text{K}))/x(12\ \text{K})$ for a, b and c lattice parameters (x). The respective values of relative thermal expansion are almost the same for a and b parameters. The relative expansion along the c-direction is not pronounced until $T = 175$ K and comes to be about five times lower at $T = 290$ K in comparison with the relative expansion along the a- and b-directions. The small thermal changes in the c parameter have to be emphasized for the YbP_3O_9 structure (figure 3(c)).

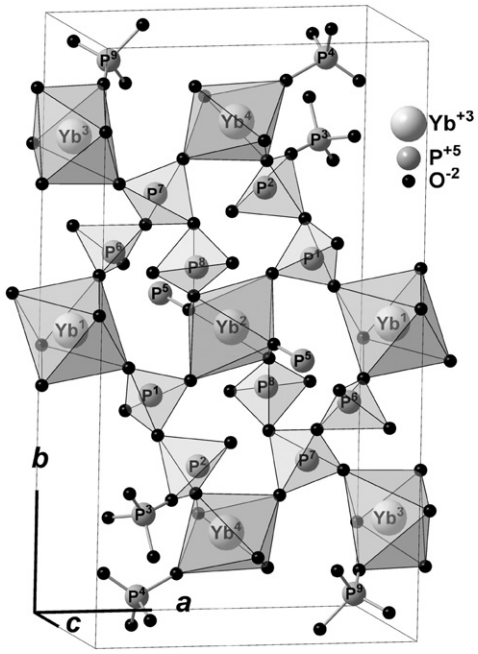

Figure 2. Structure of ytterbium metaphosphate [2].

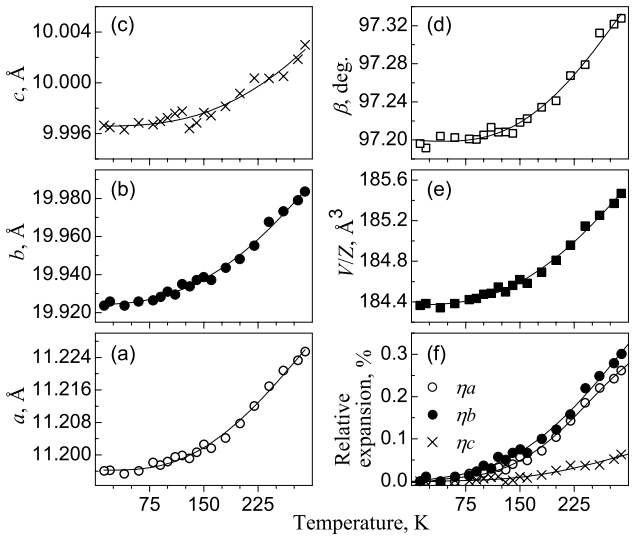

Figure 3. Temperature dependences of lattice parameters a, b, c and β (frames (a)–(d)), cell volume per formula unit V/Z ($Z = 12$, frame (e)) and relative expansion (frame (f)) of YbP_3O_9 as functions of temperature in the 12–290 K range. Relative expansion is determined as $\eta x(T) = 100\% \times (x(T) - x(12\text{ K}))/x(12\text{ K})$, where $x = a, b, c$.

4. Results of the luminescence spectral-kinetic study

The structure of ytterbium metaphosphate implies a rather large distance and a reduced interaction between Yb^{3+} ions that make this material attractive for the spectroscopic study of Yb^{3+} luminescence.

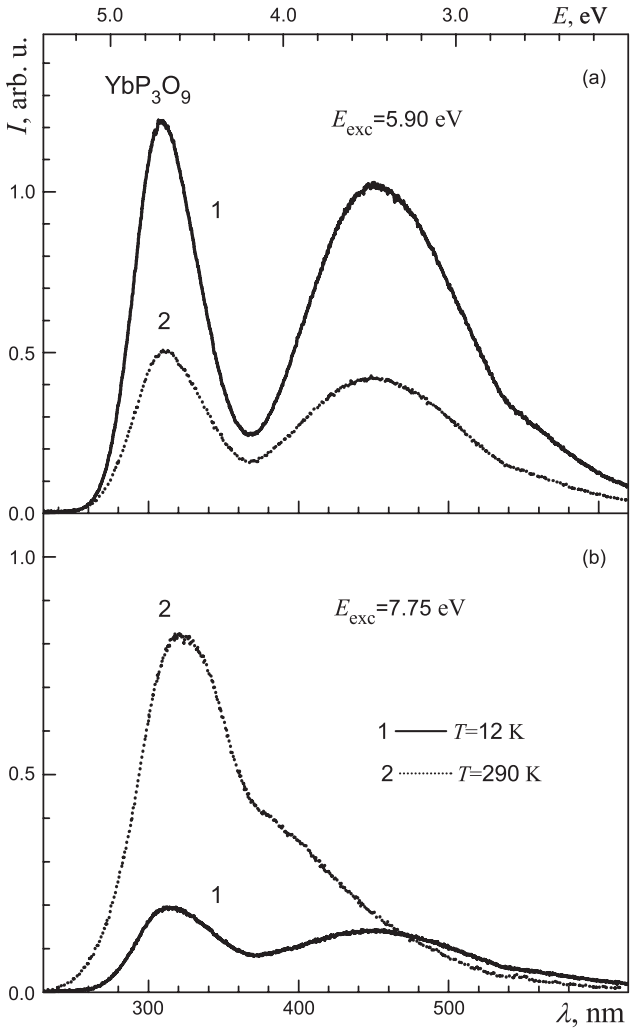

Figure 4. Emission spectra of YbP_3O_9 upon excitation in the range of Yb^{3+} charge transfer (frame (a)) and electron–hole pair creation (frame (b)) at $T = 12$ K (curves 1) and $T = 290$ K (curves 2).

Table 1. Results of the polynomial $F(T) = A_0 + A_1T^2 + A_2T^3 + A_3T^4$ fit of YbP_3O_9 lattice parameters in the 12–290 K temperature range.

	a (Å)	b (Å)	c (Å)	β (deg)
A_0	11.1963	19.9244	9.9966	97.199
A_1	-9.47×10^{-8}	2.69×10^{-7}	1.14×10^{-9}	-1.07×10^{-6}
A_2	3.05×10^{-9}	2.73×10^{-9}	3.57×10^{-10}	1.66×10^{-8}
A_3	-5.21×10^{-12}	-4.13×10^{-12}	-3.92×10^{-13}	-2.57×10^{-11}

Besides the characteristic Yb^{3+} $^2F_{5/2} \rightarrow {}^2F_{7/2}$ infrared luminescence, emission in the UV–visible range has been revealed for YbP_3O_9 metaphosphate upon excitation within the 5–11 eV range at $T = 12$–290 K. The spectra of UV–visible emission have complex profiles containing several broad bands within the 200–650 nm range (figure 4). The most intensive emission

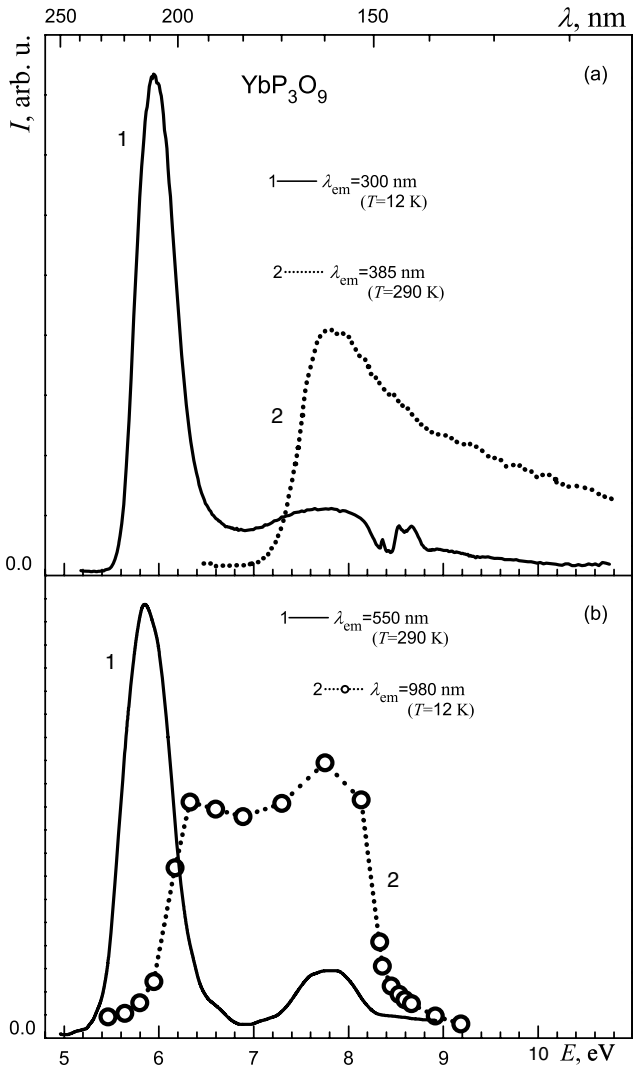

Figure 5. The excitation spectra measured for short-wavelength (frame (a)) and long-wavelength (frame (b)) luminescence of YbP_3O_9 at $T = 12$ and 290 K.

bands are peaked at 308 and 450 nm (figure 4(a)), revealing similar excitation spectra with the maximum at around 5.94 eV (figure 5(a), curve 1) at $T = 12$ K. Upon excitation in the 5.94 eV absorption peak, the 308 nm and 450 nm emission bands prevail (figure 4(a)) and show single exponentional decay kinetics (figure 6, curve 2), with a decay time constant varying from 97 to 36 ns while the temperature changes in the 12–290 K interval (figure 7, triangles).

The position of the main excitation maximum (5.94 eV) as well as the decay time values for YbP_3O_9 emission around 308 and 450 nm are close to those reported for the charge transfer luminescence (CTL) of Yb^{3+} ions in $LuPO_4$:Yb, YPO_4:Yb and $LiYP_4O_{12}$:Yb phosphates [11–14]. The energy distance between the 308 and 450 nm maxima of YbP_3O_9 UV–visible emission (1.27 eV) is well matched with the splitting of the Yb^{3+} ^2F term. Spectral-kinetic characteristics that are revealed for the emission bands of YbP_3O_9 around 308 and

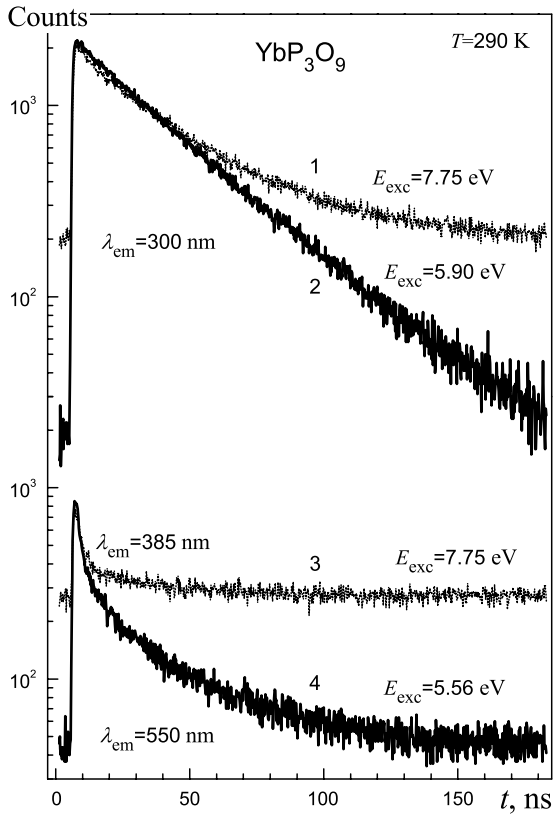

Figure 6. Decay kinetics of UV–visible emission from YbP_3O_9 metaphosphate upon excitation in Yb^{3+} CT (curves 2, 4) and excitonic (curves 1, 3) absorption range at $T = 290$ K.

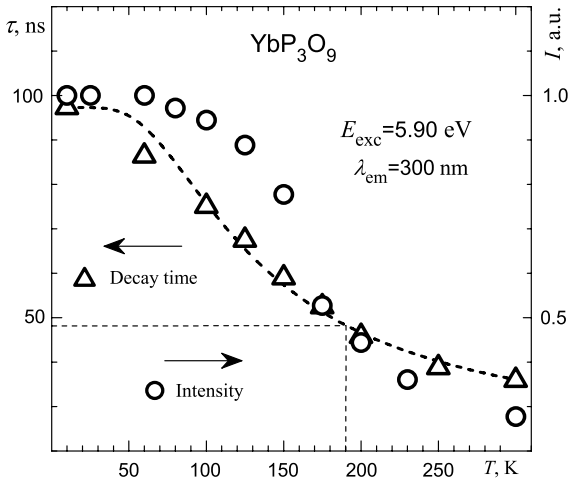

Figure 7. Temperature dependence of the intensity and the decay time of 300 nm emission from YbP_3O_9 upon excitation in the Yb^{3+} CT absorption band. A Mott fit for the decay time is presented by the dashed line.

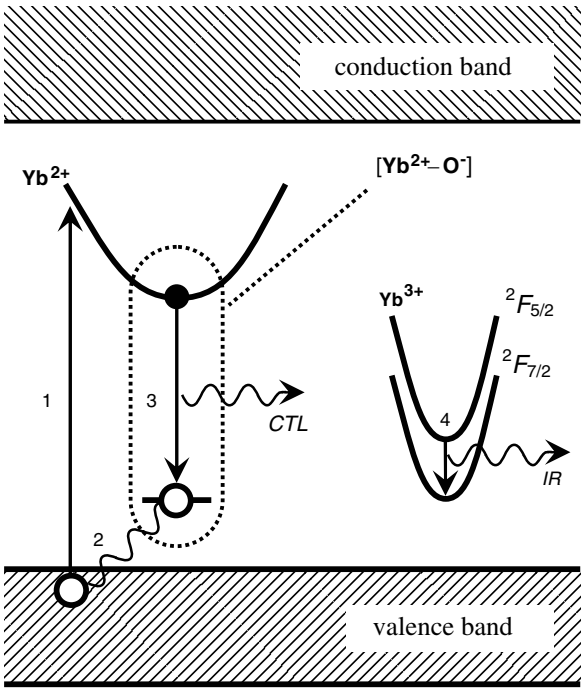

Figure 8. The schematic diagram depicts the relaxation processes in YbP_3O_9 after electron $O^{2-} \rightarrow Yb^{3+}$ transfer (1) resulted in Yb^{2+} and O^- hole delocalized around it. After hole localization (2), radiative recombination (3) occurs within a $[Yb^{2+}–O^-]$ cluster, giving rise to CT luminescence (CTL) and restoring the Yb^{3+} ion either in the $^2F_{7/2}$ state or in the $^2F_{5/2}$ state. Further radiative relaxation of Yb^{3+} $^2F_{5/2}$ (4) gives rise to infrared (IR) emission of Yb^{3+} around 980 nm.

450 nm allow us to attribute the excitation maximum at 5.94 eV (figure 5(a), curve 1) to the absorption implicating electron transfer from the O^{2-} ligand to the Yb^{3+} ion within YbO_6 octahedra in YbP_3O_9. Such electron transfer (figure 8, transition 1) causes the formation of the excited Yb^{3+} CT state $[Yb^{2+}–O^-]$ involving the central Yb^{2+} ion and the hole delocalized over the ligands around Yb^{2+} [13]. The delocalized (mobile) hole has most likely to be localized (figure 8, transition 2) before the occurrence of its radiative recombination with the electron from Yb^{2+}. The UV–visible emission bands peaked at 308 and 450 nm (figure 4(a)) correspond to Yb^{3+} CTL originating from the radiative recombination (figure 8, transition 3) of an electron at Yb^{2+} with the hole localized on the ligand. It is difficult to consider relaxation of the excited Yb^{3+} CT state $[Yb^{2+}–O^-]$ in the frame of a band model because of possible ion displacement due to interaction of the polarized ligands with the Yb^{2+} ion. Therefore, the Yb^{2+} ion and the hole delocalized over the ligands around it were proposed to be considered as a Yb^{2+} CT *cluster* [14]. After relaxation of the Yb^{3+} CT state, the Yb^{3+} ion appears in either the $^2F_{7/2}$ ground state or the $^2F_{5/2}$ excited state, and further $^2F_{5/2} \rightarrow {}^2F_{7/2}$ radiative transition (figure 8, transition 4) gives rise to infrared Yb^{3+} emission at around 980 nm. Hence, the CTL and $^2F_{5/2}$–$^2F_{7/2}$ emission of Yb^{3+} ion are considered to be two consequent radiative processes.

To plot the VUV excitation spectra for Yb^{3+} $^2F_{5/2}$–$^2F_{7/2}$ emission at $T = 8$ K (figure 5(b), curve 2), the luminescence spectra measured upon the corresponding excitation were integrated within the 1.13–1.39 eV range. The maxima (6.32 and 7.75 eV) of the excitation efficiency revealed within the 5.4–9.2 eV range for the infrared Yb^{3+} $^2F_{5/2}$–$^2F_{7/2}$ emission do not coincide with the maximum (5.94 eV) of Yb^{3+} CT absorption (figure 5). Such a difference in the

locations of the main excitation maxima for Yb^{3+} CTL and $^2F_{5/2}$–$^2F_{7/2}$ emission points out the presence of some additional mechanisms for the population of the Yb^{3+} $^2F_{5/2}$ state upon excitation in the UV–VUV range.

The CTL of Yb^{3+} is observed for YbP_3O_9 not only upon direct Yb^{3+} CT absorption, but also upon excitation at higher energies ($E > 6.4$ eV, figure 5(a), curve 1). Excitation at 7.75 eV gives rise to emission in two dominant Yb^{3+} CTL bands at $T = 12$ K (figure 4(b), curve 1). The temperature increase causes considerable changes in the emission spectrum of YbP_3O_9 upon excitation above 7.5 eV (figure 4(b), curve 2).

To clarify the origin of the emission rising within the 240–500 nm range upon a temperature increase, the excitation spectrum and decay kinetics were studied for the emission at around 385 nm where the contribution of Yb^{3+} CTL is relatively small. The excitation spectrum of 385 nm emission clearly shows a threshold at 7.2 eV and a maximum at about 7.8 eV at $T = 290$ K (figure 5(a), curve 2). Upon 7.75 eV excitation, the slow component (>10 μs) prevails in the decay kinetics of 385 nm emission at $T = 290$ K (figure 6, curve 3), while the decay kinetics of 300 nm emission additionally shows a characteristic 36 ns decay component (figure 6, curve 1), indicating a contribution from Yb^{3+} CTL in this range. The threshold at 7.2 eV that is revealed in the excitation spectrum of 385 nm emission may correspond to the creation of electron–hole pairs in the YbP_3O_9 host. At $T = 12$ K, the CTL of Yb^{3+} prevails upon excitation within the energy range of electron–hole pair creation (figure 4(b), curve 1), i.e. the carriers tend to be localized around Yb^{3+} ions, forming excited Yb^{3+} CT states at low temperature. Carrier migration is intensified at higher temperatures, and the localization of carriers beyond the YbO_6 octahedra (figure 2) comes to be more probable, resulting in some kind of defect-related or excitonic emission with maximum intensity around 385 nm (figure 4(b), curve 2).

The excitation maxima of Yb^{3+} $^2F_{5/2}$–$^2F_{7/2}$ infrared emission (figure 5(b), curve 2) and the excitation band corresponding to the creation of electron–hole pairs (figure 5(a), curve 2) overlap within the 7–9 eV range. As has already been supposed [15], the infrared Yb^{3+} $^2F_{5/2}$–$^2F_{7/2}$ emission may be excited via the interaction of Yb^{3+} ions with electron–hole pairs.

A fast decay component ($\sim$1 ns) is revealed for the long-wavelength emission (385–550 nm) of YbP_3O_9 upon excitation within the 5–11 eV range (figure 6, curves 3, 4). Fast decay is most pronounced for the emission at 550 nm, where a hyperbolic-like profile of the decay kinetics (figure 6, curve 4) is revealed. Such decay kinetics is characteristic for the recombinational radiative processes and may also point to nonradiative decay of the excited state. Emission at 550 nm is efficiently excited in the range of Yb^{3+} CT (5.86 eV) and in the 7.8 eV peak (figure 5(b), curve 1) where the absorption of YbP_3O_9 is high. The penetration depth of the excitation quanta is small in the range of strong absorption, and surface defects affect the emitting centers in this case. Thus, the luminescence of YbP_3O_9 around 550 nm originates most likely from the emitting centers located at the surface. A fast component in the decay kinetics of YbP_3O_9 emission may appear due to the interaction of emitting centers with surface defects.

Due to the thermostimulated intensification of carrier mobility, the probability of their escape from YbO_6 octahedra increases and the formation of excited Yb^{3+} CT states is reduced at high temperature. As a result, the intensity of Yb^{3+} CTL decreases by about three times, while the temperature changes within the 12–290 K range (figure 7, circles). To exclude the contribution from the excitonic or defect-related emission overlapping spectrally with Yb^{3+} CTL, the temperature dependence of the decay time constant (figure 7, triangles) has been analyzed for Yb^{3+} CTL. The characteristic ($\sim$10 ns) exponentional kinetics of Yb^{3+} CTL decay (figure 6, curve 2) provides the possibility of distinguishing its contribution against the

slow (>10 μs) excitonic (figure 6, curve 3) or fast (∼1 ns) defect-related (figure 6, curve 4) emission and reproducing the thermo-stimulated decay of Yb^{3+} CT states. The quenching temperature of Yb^{3+} CTL has been estimated to be about 190 K for YbP_3O_9 metaphosphate. The temperature value corresponding to the half-maximum of the decay time (figure 7) has been considered for this purpose. Temperature quenching of Yb^{3+} CTL may occur (i) due to thermally activated cross-over from the excited Yb^{3+} CT state to the Yb^{3+} ^2F_j states [15] or (ii) via ionization involving most likely hole escape from the Yb^{3+} CT state to the valence band [13].

The temperature dependence of the decay time of Yb^{3+} CTL was approximated using Mott's law (figure 7, dashed curve). An attempt has been made to estimate the activation energy for the thermo-stimulated decay of the Yb^{3+} CT state. The value 23.2 meV was obtained from the fit of the decay time dependence. One may suppose such a small value (23.2 meV) of activation energy to reproduce the energy barrier between the localized and delocalized (mobile) hole involved in the Yb^{3+} CT state. Ionization of the Yb^{3+} CT state is expected to occur via hole escape into the valence band [13]. Quenching of Yb^{3+} CTL has been supposed to be caused by the recombination of carriers with the hole or electron involved in the Yb^{2+} CT cluster [14]. The probability of such quenching should be higher for the case of a mobile hole delocalized over the ligands around the Yb^{2+} ion.

The excitation spectrum of the Yb^{3+} CTL shows the narrow troughs within the 8.2–9 eV range (figure 5(a), curve 1) at T = 12–290 K. Such troughs are not revealed in the excitation spectrum of 385 nm emission (figure 5(a), curve 2). To clarify the origin of the absorption processes reducing the formation of the excited Yb^{3+} CT state, a detailed analysis of YbP_3O_9 emission has been performed in the VUV range upon excitation within the 8–10 eV range. The interconfigurational Yb^{3+} $4f^{13} \rightarrow 4f^{12}5d$ transitions have been estimated for the YPO_4 host to start 2.3 eV above the Yb^{3+} CT absorption [16]. The difference of 2.3 eV fits the energy distance between the Yb^{3+} CT absorption peak (5.94 eV) and the first narrow trough (8.33 eV) revealed within the 8.2–9 eV range in the excitation spectrum of Yb^{3+} CTL from YbP_3O_9 (figure 5(a), curve 1). The formation of the excited Yb^{3+} CT state may compete with Yb^{3+} $4f^{13} \rightarrow 4f^{12}5d$ absorption upon excitation within the 8–10 eV. However, there was no reliable luminescence signal revealed in the 155–200 nm range from YbP_3O_9 upon excitation in the 8–10 eV range.

Further studies of $Y_{1-x}Yb_xP_3O_9$ concentration series may clarify the origin of the absorption features revealed for YbP_3O_9 in the 8–10 eV range. To reveal the contribution of Yb^{3+} absorption, a luminescence study should be performed for YP_3O_9, which is isostructural to YbP_3O_9 [2]. The influence of surface defects is expected to be suppressed in the case of a diluted $Y_{1-x}Yb_xP_3O_9$ system due to the increase in penetration depth for the excitation quanta within the transparency range of the YP_3O_9 host.

5. Conclusions

The XRD studies show the YbP_3O_9 structure to be monoclinic ($P2_1/c$ space group) within the 12–290 K temperature range. The thermal expansion of the YbP_3O_9 unit cell within the 12–290 K range occurs mostly due to lattice changes along the a- and b-directions. Small thermal changes in the c parameter have been revealed for the YbP_3O_9 structure.

Charge transfer luminescence originating from the Yb^{3+} ion has been revealed for ytterbium metaphosphate (YbP_3O_9) at T = 12–290 K. At higher temperatures, the carrier migration is intensified and the efficiency of Yb^{3+} CTL decreases by about three-fold while the temperature changes within the 12–290 K range. The carriers in YbP_3O_9 tend to be localized beyond the YbO_6 octahedra at room temperature, while formation of the Yb^{3+} CT state prevails

at $T = 12$ K. The activation energy for the thermo-stimulated decay of the Yb^{3+} CT state has been estimated to be 23.2 meV for YbP_3O_9. This value may correspond to the energy barrier between the states of localized and delocalized (mobile) holes involved in the Yb^{2+} CT cluster. Formation of the excited Yb^{3+} CT state may compete with Yb^{3+} $4f^{13} \rightarrow 4f^{12}5d$ absorption upon excitation within the 8–10 eV range, but further studies are necessary to clarify the origin of the absorption features revealed for YbP_3O_9 in the 8–10 eV range.

Acknowledgments

The authors appreciate the assistance of Andreas Berghaeuser during the low-temperature XRD measurements. The HASYLAB (DESY) support of Powder Diffractometer (Beamline B2) and SUPERLUMI experiment (Beamline 1) is gratefully acknowledged.

References

[1] Hong H Y-P 1974 *Acta Crystallogr.* B **30** 468
[2] Hong H Y-P 1974 *Acta Crystallogr.* B **30** 1857
[3] Goldner P, Schaudel B and Prassas M 2002 *Phys. Rev.* B **65** 54103
[4] Martin R A, Salmon Ph S, Fischer H E and Cuello G J 2003 *Phys. Rev. Lett.* **90** 18501
[5] Nakazawa E and Shionoya S 1970 *Phys. Rev. Lett.* **25** 1710
[6] Knapp M, Baehtz C, Ehrenberg H and Fuess H 2004 *J. Synchrotron Radiat.* **11** 328
[7] Ihringer J and Kuester A 1993 *J. Appl. Crystallogr.* **26** 135
[8] Knapp M *et al* 2004 *Nucl. Instrum. Methods* A **521** 565
[9] http://www-llb.cea.fr/fullweb/fp2k/fp2k.htm
[10] Zimmerer G 1991 *Nucl. Instrum. Methods* A **308** 178
[11] Nakazawa E 1978 *Chem. Phys. Lett.* **56** 161
[12] Nakazawa E 1979 *J. Lumin.* **18/19** 272
[13] van Pieterson L 2001 Charge transfer and $4f^n$–$4d^{n-1}5d$ luminescence of lanthanide ions *PhD Thesis* Utrecht University
[14] Stryganyuk G *et al* 2007 *J. Phys.: Condens. Matter* **19** 036202
[15] Kamenskikh I A *et al* 2005 *J. Phys.: Condens. Matter* **17** 5587
[16] Dorenbos P 2003 *J. Phys.: Condens. Matter* **15** 8417